ATL-COM-PHYS-2000-030
March 8, 2001

Physics in ATLAS at a possible upgraded LHC

G. Azuelos[a], D. Benchekroun[b], O. Çakır[c], F. Gianotti[d], J.-B. Hansen[d], I. Hinchliffe[e], C. Leroy[a], R. Mehdiyev[a,j], F.E. Paige[f], G. Polesello[g], H. Stenzel[h], S. Tapprogge[i], Z. Usubov[k], L. Vacavant[e]

[a] *U. of Montreal, Montreal, Canada*
[b] *Univ. Hassan II Casablanca-Maarif, Casablanca. Morocco*
[c] *U. of Ankara, Turkey*
[d] *CERN, Geneva, Switzerland*
[e] *Lawrence Berkeley National Laboratory, Berkeley, CA*
[f] *Brookhaven National Laboratory, Upton, NY*
[g] *INFN, Sezione di Pavia, Pavia, Italy*
[h] *Max-Planck-Institut fur Physik, Munich, Germany*
[i] *HIP, Helsinki, Finland*
[j] *Institute of Physics, Academy of Sciences of Azerbaijan, Baku, Azerbaijan*
[k] *Joint Institute for Nuclear Research, Dubna, Russia*

Abstract

The impact on the physics capabilities of the ATLAS detector of possible LHC upgrades is discussed. A doubling of the LHC energy or an increase in the luminosity by a factor of ten are considered. Both upgrades significantly enhance the physics capabilities of ATLAS. In general, the energy upgrade is more powerful since the pile-up of minimum bias events at higher luminosity impacts the physics performance of ATLAS in some areas.

1 Introduction

Four basic scenarios for High Energy/luminosity pp colliders are considered. The higher luminosity operation would correspond to a bunch spacing of 12.5 ns.

- A The approved LHC, *i.e.* 14 TeV and luminosity of 10^{34} cm^{-2} sec^{-1}
- B 14 TeV and luminosity of 10^{35} cm^{-2} sec^{-1}
- C 28 TeV and luminosity of 10^{34} cm^{-2} sec^{-1}
- D 28 TeV and luminosity of 10^{35} cm^{-2} sec^{-1}

Note that, while scenario B represents a realistic upgrade scenario for the LHC, scenarios C and D are more speculative but are provided for comparison purposes. The impact of the upgrades on detector performance has not been assessed in detail but a few general remarks are appropriate. The higher luminosity has a severe impact. In the case of the Inner Detector, the TRT would need to be replaced due to the high occupancy. Radiation damage would imply replacement or removal of the pixels and part of the SCT. Removal would imply loss of electron identification and b-tagging capability. Calorimeter performance is not expected to be impacted significantly in the central region; some of the tile scintillating fibers may need to be replaced. The forward calorimeter (FCAL) could be compromised by space-charge effects which might be compensated by increasing the voltage. More shielding will be required for the forward muon system which will reduce the fiducial region. The reduced bunch spacing at very high luminosity has a severe impact on the front-end electronics, trigger and DAQ components. For example, the front end pipeline buffers would be incompatible with the latency needed for the level-1 trigger. The level-1 muon trigger could also be compromised by increased occupancy in the RPC's and TGC's.

The ATLAS B-physics programme [1] does not benefit from the energy and luminosity upgrades. The programme is accomplished primarily at low luminosity and as the total B cross section increases only slightly at the higher energy the energy upgrade will have little impact. Similarly the top production rate is very large and, possibly apart from rare decay modes, the physics will be fully exploited at design energy/luminosity.

Physics processes involving the production of high-mass systems have cross-sections that rise rapidly with energy. One should expect therefore that, if the impact of upgrades is assessed in terms of mass reach for new particles, the energy upgrade will be more powerful. This general conclusion will be substantiated by the preliminary studies that are presented. It should be noted, however, that the luminosity upgrade has the capability to significantly enhance the LHC capability.

2 QCD studies and searches for compositeness

For QCD studies at an upgraded LHC, a comparison of the reach in jet transverse momenta was carried out. Using a NLO calculation of the inclusive jet cross section [2], the expected number of events with a jet above a transverse energy threshold is shown in Figure 1. Requiring that dN/dE_T be greater than 10 events/(100 GeV), the accessible E_T is shown in Table 1. This comparison clearly shows the advantage of increasing the center-of-mass energy to 28 TeV over a 10-fold increase in luminosity. In the former case, the reach extends by about 2.7 TeV, larger by a factor of more than 4 than in the latter case. As the measurements involve the calorimeters only and only jets in the TeV range are of interest the performance is not expected to be degraded significantly at the highest luminosity.

Signals for quark compositeness should reveal themselves in deviations of the high energy part of the jet cross-section from the QCD expectation. The angular distribution of dijet pairs provides an independent

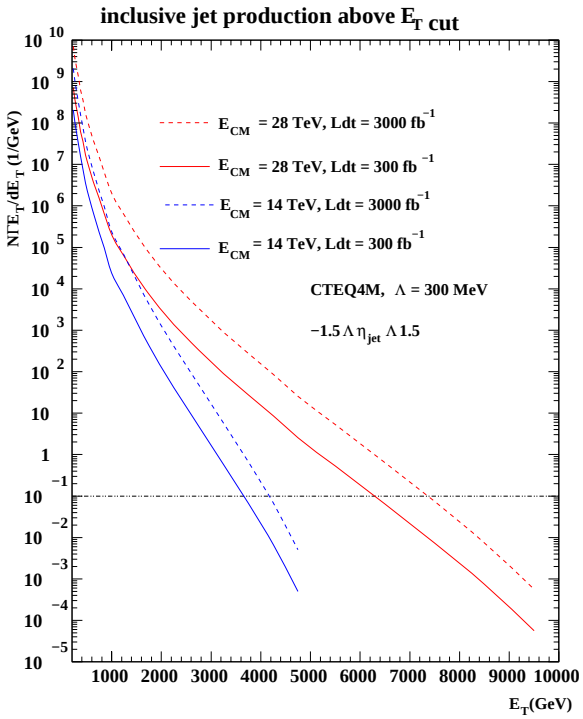

Figure 1: Expected number of events with a jet of transverse energy larger than E_T for the four scenarios studied.

scenario	14 TeV 300 fb^{-1}	14 TeV 3000 fb^{-1}	28 TeV 300 fb^{-1}	28 TeV 3000 fb^{-1}
max E_T (TeV)	3.6	4.2	6.2	7.4

Table 1: The maximum value of jet transverse momentum that is accessible in various LHC energy/luminosity scenarios.

tool and is less sensitive to possible non-linearities in the calorimeter response (see Section 21.5 of Ref [1] for more details on the methodology). Figure 2 shows the distribution for dijet events in the variable $\chi = (1+|\cos\theta|)/(1-|\cos\theta|)$, where θ is the angle between a jet and the beam in the center-of-mass frame of the dijet system. Shown is the deviation from the expected form in the Standard Model. The compositeness scales that can be probed in this manner are shown in Table 2.

scenario	14 TeV 300 fb^{-1}	14 TeV 3000 fb^{-1}	28 TeV 300 fb^{-1}	28 TeV 3000 fb^{-1}
Λ(TeV)	40	60	60	85

Table 2: The 95% confidence level limits that can be obtained on the compositeness scale Λ using the dijet angular distributions.

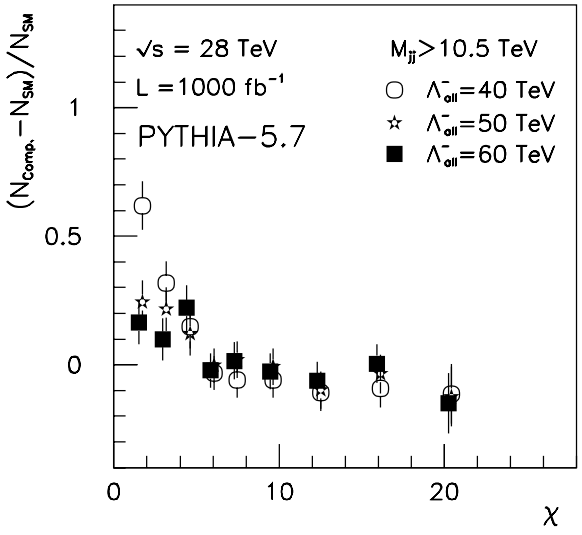

Figure 2: Deviation from the Standard Model predictions for the angular distribution of dijet pairs at 28 TeV for various values of the compositeness scale Λ. Dijet pairs are required to have invariant mass greater than 10.5 TeV.

scenario	14 TeV 100 fb^{-1}	14 TeV 1000 fb^{-1}	28 TeV 100 fb^{-1}	28 TeV 1000 fb^{-1}
$m_{\tilde{q}} \sim m_{\tilde{q}}$	2.1	2.7	3.9	4.4
$m_{\tilde{q}} = 2m_{\tilde{g}}$	2.0	2.3	2.7	4.2
$m_{\tilde{g}} \sim 2m_{\tilde{q}}$	1.9	2.2	2.9	4.1

Table 3: Comparison of the reach in squark masses in TeV in the different scenarios. In each case a nominal one year of running is assumed.

3 Supersymmetry studies

The increase in mass reach for squarks and gluinos is approximately evaluated by comparing the squark and gluino production cross-sections at 14 and 28 TeV. The primary Standard Model backgrounds, $t\bar{t}$ production and W/Z+jets increase due to the larger center of mass energy. However, this effect will be more than compensated by the harder cuts on the transverse energy flow and missing E_T in the events which can be applied compared to the analysis performed for a 14 TeV collider. The cross-section calculation was evaluated at leading order using the program PROSPINO [3]. The CTEQ4L [4] structure functions were used. Three scenarios were considered: $m_{\tilde{q}} = 2m_{\tilde{g}}$, $m_{\tilde{g}} = 2m_{\tilde{q}}$, $m_{\tilde{g}} \sim m_{\tilde{q}}$. The total cross section for the production of squarks and gluinos is given in the Figures 3, 4 and 5 as a function of the mass of the lighter sparticle be it squark or gluino.

An approximation of the reach at 28 TeV is obtained by taking the masses for which the signal cross-section is equal to the one for the maximum reachable masses at 14 TeV [1], *i.e.* around 10^{-2} pb for 100 fb^{-1}. The approximate SUSY mass reach for an integrated luminosity of 100 fb^{-1} at 28 TeV is thus: 3.9 TeV for $m_{\tilde{q}} \sim m_{\tilde{g}}$, 2.7 TeV for $m_{\tilde{q}} = 2m_{\tilde{g}}$, and 2.9 TeV for $m_{\tilde{g}} \sim 2m_{\tilde{q}}$. which corresponds to an approximate doubling of the accessible mass range. An increase in the luminosity is less powerful as can be seen from Table 3, but it still provides a mass reach 20% higher than the standard LHC scenario.

Given the large mass reach in the case of the baseline LHC, it is almost guaranteed that SUSY will be

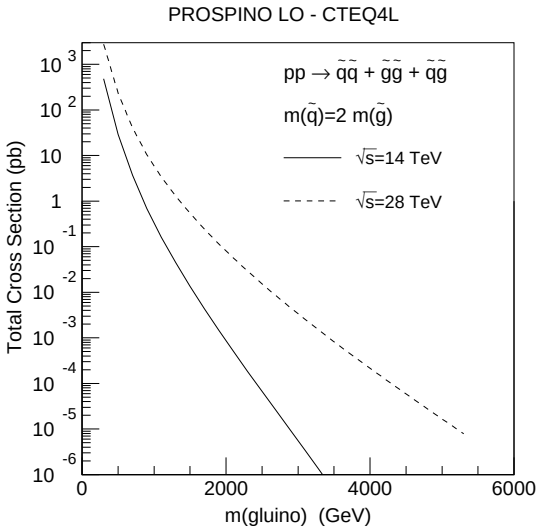

Figure 3: The total SUSY production cross section as a function of the gluino mass for the case where $m_{\tilde{q}} = 2.0 m_{\tilde{g}}$.

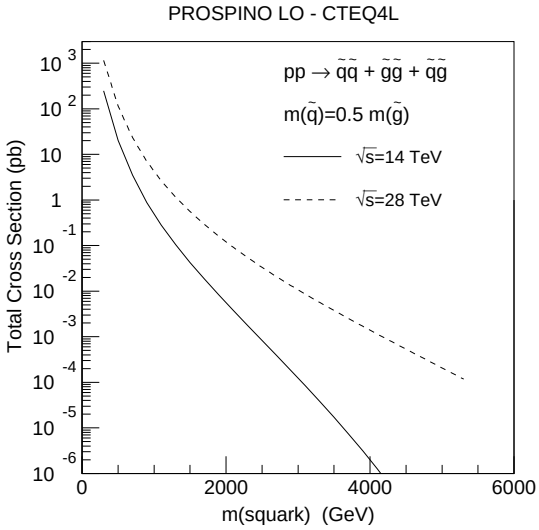

Figure 4: The total SUSY production cross section as a function of the squark mass for the case where $m_{\tilde{q}} = 0.5 m_{\tilde{g}}$.

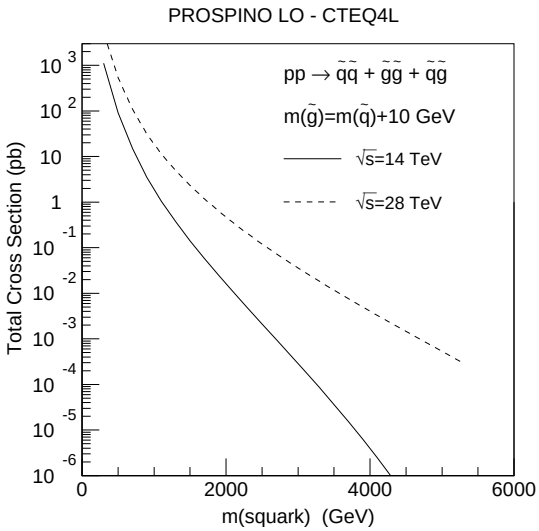

Figure 5: The total SUSY production cross section as a function of the squark mass for the case where $m_{\tilde{g}} = m_{\tilde{q}} + 10$ GeV.

discovered if it is relevant to the problem of electroweak symmetry breaking. However some studies may be limited by the available statistics. The full ATLAS capability is essential for many of these studies which will often involve e, μ and τ final states. The studies will be seriously compromised if, for example, electron identification is lost at high luminosity. For squark and gluino masses around 1 TeV, the production rate increases by approximately a factor of 10 if the machine energy is doubled so the energy and luminosity upgrades are comparable as measured by event rate. If the difficulties of operating in a higher luminosity environment cannot be overcome, the energy upgrade is more powerful. The direct production of gauginos and sleptons has a small rate and therefore could benefit from an upgrade. However a jet veto is needed to extract the signal and, as discussed in Section 4, this could be seriously compromised at increased luminosity.

In inverted hierarchy models [5], the squarks of the first two generations are much heavier than the gluinos and the top and bottom squarks. In a model of this type, the light squark production rates may be too small for them to be observed at the LHC. An energy upgrade could be sufficient to discover them.

4 Jet tagging/vetoing at higher luminosity

The presence of jets at large rapidity can be used to enhance the signal-to-background ratio in certain processes such as those involving WW fusion where the W's are emitted from quarks (see, for example, 19.2.10.1 of Ref [1]). Similarly the absence of jets at central rapidity can be used to enhance processes involving the production of particles with only electroweak charges relative to the production of strongly coupled particles (see, for example, 19.2.10.2 of Ref [1]). As the luminosity increases both of these selections are expected to become less useful as the pile-up of additional events can cause jets to appear in these regions and degrade the jet measurements.

For a particle level study using PYTHIA, a grid of 0.1 x 0.1 in $\eta \times \phi$ was used. A Poisson average of 23 or 250 minimum bias events, for the two luminosity cases 10^{34} and 10^{35} cm^{-2} sec^{-1}, were generated and the energy in each bin of $\eta - \phi$ was summed. To approximate the effect of the shape of the calorimeter response, for each of the 19 beam crossings before the triggered event, the corresponding number of minimum bias

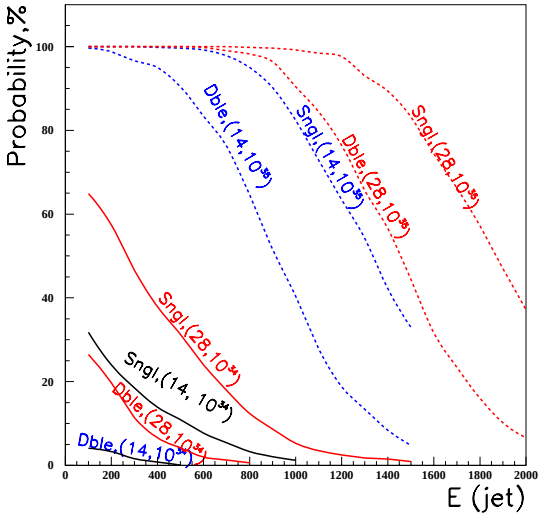

Figure 6: Probability of fake forward jet tagging from pile-up, for nominal and very high luminosities, at 14 and 28 TeV as a function of the jet energy.

events were produced and they contributed a negative part (1/19th) of their energy to the calorimeter bins. Jets were then found using the standard jet finder with cone size $\Delta R = 0.4$ and assigned to ranges of rapidity

- Forward: $\eta > 2.5$
- Backward: $\eta < -2.5$
- Central: $|\eta| < 2.$

A single tag is defined as an event with either a forward or backward jet; a double tag has both. The probability of an event having either a single or double jet tag is shown in Figure 6 as a function of the jet energy. The probability of an event having an additional central jet is shown in Figure 7.

In conclusion, at a luminosity of 10^{35} cm^{-2} sec^{-1} the pile up of minimum bias events renders forward jet tagging and central jet vetoing very difficult. The performance that is assumed here may be too pessimistic as it may be possible to reduce the pile-up noise in the LAr calorimeter by using optimal filtering techniques at the upgraded luminosity [7] and optimizing the jet algorithm. This tagging result has implications for strong WW scattering signals as is now discussed.

5 Strongly coupled WW system

If there is no light Higgs boson, then general arguments [8] imply that scattering of electroweak gauge bosons at high energy will show structure beyond that expected in the Standard Model. In order to explore such signals it is necessary to measure final states of pairs of gauge bosons with large invariant mass. Production of W^+W^+ pairs has been studied and two models have been considered:

- A Higgs boson of mass 1 TeV (as a reference point).
- WW production with K-matrix unitarization.

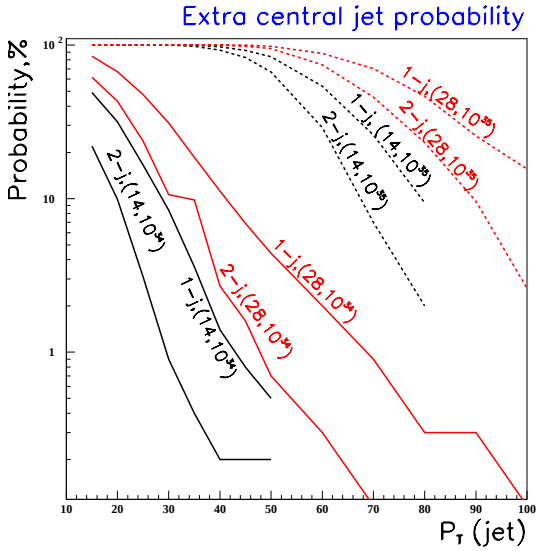

Figure 7: Probability of observing extra central jets from pile-up for nominal and very high luminosities, at 14 and 28 TeV as a function of jet transverse energy.

Backgrounds arise from gauge boson pairs produced by electroweak and gluon exchange diagrams [1]. Here the promising $\ell^+\ell^+\nu\nu$ final state arising from W^+W^+ production is studied. The analysis cuts are essentially the same as in [1], except that for the 28 TeV case, the leptonic cuts were adjusted:

- $\Delta\phi(\ell\ell) < -0.5 \rightarrow \Delta\phi(\ell\ell) < -0.8$
- $\Delta p_t(ll) > 0 \rightarrow \Delta p_t(ll) > 100$ GeV.
- $E_T^{miss} > 40$ GeV $\rightarrow E_T^{miss} > 50$ GeV

The jet tagging and vetoing cuts were varied as a function of the energy and luminosity as shown in table 4. It is clear from the above discussion that forward jet tagging and central jet veto are not useful at very high luminosities. Two forward tagging jets with energies above the amount shown in the table were required and events were vetoed if there was a central jet with transverse momentum greater than the indicated amount. Table 5 shows the number of events expected and their significances for a typical set of cuts, for 300 fb^{-1} at nominal luminosity and 3000 fb^{-1} at very high luminosity at 14 and 28 TeV. In the case of ultra high luminosity both leptons are required to be muons. The pessimistic conclusions regarding an increase in luminosity that can be drawn from table 5 should be treated with caution. It may be possible to reduce the effects of pile up by improving filtering and optimising the jet tagging. Nevertheless, in order to exploit the luminosity increase at 14 TeV, it is essential that electrons be included; in this case the significance would increase by approximately a factor of two.

The increase in energy to 28 TeV would enhance considerably the study of high mass vector boson pair production, even in a non-resonant scenario. The study of the signal could be pushed from a limit of about 1 TeV in the invariant mass of the WW system to around 1.5 TeV. Figures 8 and 9 show the signal and background distributions as a function of the invariant mass formed from the two leptons and the missing transverse momentum (*c.f.* Figure 19-110 of [1]). In spite of the apparent increase in statistical significance, the systematic errors are likely to be very high since the shapes of the backgrounds and signal are similar and the signal to background ratio is less than one in the very high luminosity cases due to the reduction in the

	300 fb^{-1} 14 TeV	3000 fb^{-1} 14 TeV	300 fb^{-1} 28 TeV	3000 fb^{-1} 28 TeV
Forward tag p	300	800	600	1000
Forward tag p_T	90	90	150	150
Central veto	40	70	60	100

Table 4: Momentum of the two forward jets required for tagging and the transverse momemtum of the central jets used for vetoing in GeV for the various energies and luminosities in the study of W^+W^+ final states. In the case of the tagging jets the transverse momenta (total momenta) are also required to be smaller(greater) than the value shown.

Model	300 fb^{-1} 14 TeV	3000 fb^{-1} 14 TeV	300 fb^{-1} 28 TeV	3000 fb^{-1} 28 TeV
Background	6.3	64	27.5	251
K-matrix Unitarization	12.7	26.6	82	324
Significance	2.9	2.8	7.8	13.5
Higgs, 1 TeV	6.2	13	29.8	100
Significance	1.7	1.5	3.9	5.3

Table 5: Numbers of reconstructed events for models of a strongly coupled Higgs sector and for the background in various LHC energy/luminosity scenarios. The significance was computed as $S/\sqrt{S+B}$.

jet tagging capability. The comparisons of signals should be done with many different choices of cuts so as to verify the dependence on the cuts and constrain the systematics. This analysis can only be an estimate of the reach. At high luminosities a good understanding of jet reconstruction and backgrounds will be needed.

Other signals such as excesses in the production of WZ final states would also benefit from increased energy/luminosity. The W^+W^+ channel has no contribution from $q\overline{q}$ fusion, but other di-boson pair signals will have a significant contribution from this process, which does not require forward jet tagging (see section 21.2.1.1 of Ref. [1]).

6 Extra dimensions

One of the possible signals for large extra dimensions is the production of jets or photons in association with missing transverse energy. The former channel is more sensitive so will be considered here. The background is dominated by the final state $Z(\rightarrow \nu\nu) + jets$ [9].

In order to assess the impact of the possible upgrades a study using ATLFAST was made. The signal is characterized by two parameters, the number of extra dimensions δ and the scale M_D characterizing the scale of gravity. Table 6 shows the maximum value of M_D that can be detected for a given value of δ in the four scenarios.

It can be seen from the table that doubling the LHC energy to 28 TeV approximately doubles the reach in M_D for any value of δ. An increase in the integrated luminosity by a factor of 10 raises the reach by approximately 30%. If a signal is observed at 14 TeV, the energy increase is such that model dependent signals can be expected to be observed at 28 TeV. Such observations would therefore provide valuable insight into the dynamics of the underlying theory. Detector performance is not expected to be critical as events with jets and missing energy in the TeV range are relevant for this search.

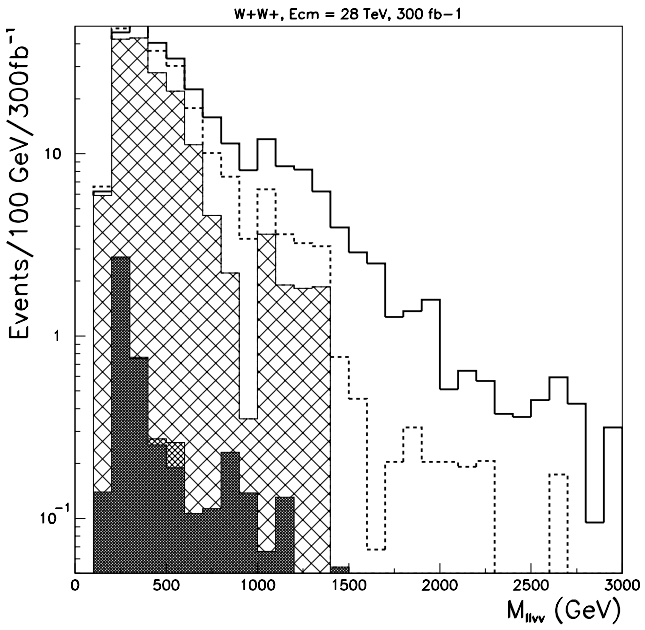

Figure 8: Signals from strong WW scattering at 28 TeV and 300 fb^{-1} of integrated luminosity. Event rates are shown as a function of the invariant mass of the $\ell\ell E_T^{miss}$ system. The backgrounds are shown as histograms, from inside to outside (or darker to lighter): WZ continuum: W pairs (transverse) from gluon exchange diagrams: W pairs (transverse) from electroweak (γ and Z exchange) diagrams. The possible signals are: continuous line, K-matrix unitarization: dashed line: Higgs, 1 TeV.

δ	14 TeV 100 fb^{-1}	14 TeV 1000 fb^{-1}	28 TeV 100 fb^{-1}	28 TeV 1000 fb^{-1}
2	9	12	15	19
3	6.8	8.3	11.5	14
4	5.8	6.9	10	12

Table 6: 5 σ discovery limits that can be achieved on M_D, in TeV, as a function of the number of extra dimensions (δ) for various values of energy and integrated luminosity.

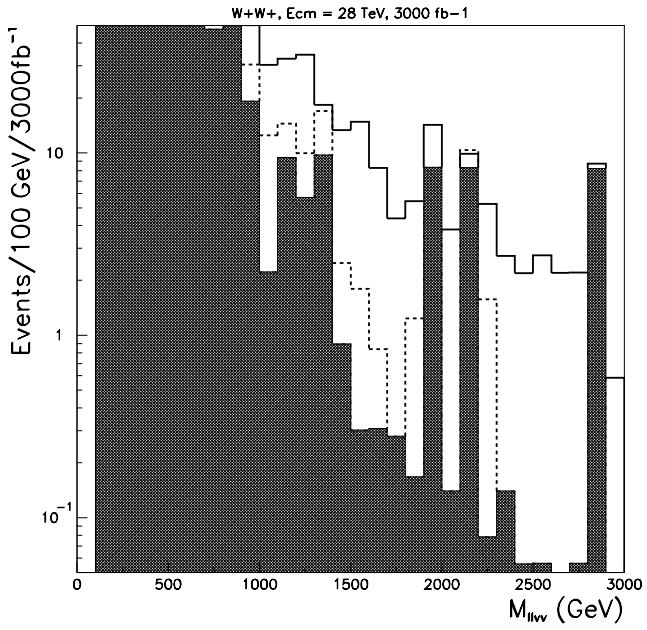

Figure 9: Same as figure 8 except for 3000 fb^{-1} of integrated luminosity.

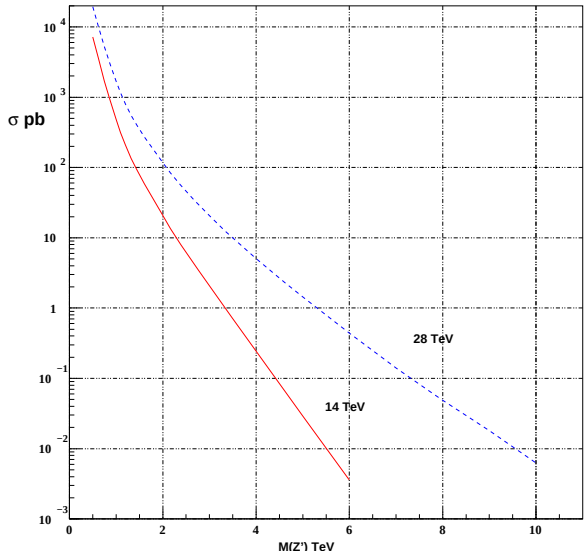

Figure 10: Production rate for $Z' \to \mu^+\mu^-$ at 14 and 28 TeV as a function of the Z' mass.

7 Searches for New Gauge Bosons

As an example of the impact of the possible upgrades, Figure 10 shows the production rate for $\mu^-\mu^+$ final states arising from the decay of a Z' gauge boson with the same couplings to quarks and leptons as the Standard Model Z as a function of the mass of the Z'. The final state e^+e^- is not considered, because it is more difficult to exploit at the highest luminosity particularly if the tracker is not upgraded. The calorimeter can still be used to detect the channel but the signs of the electrons cannot be determined and measurements of asymmetries cannot be undertaken. If this channel were included and had the same acceptance as the muon channel, the mass reach would increase by approximately 20%.

The discovery limit for gauge bosons in this channel is given in Table 7 from which it can be seen that the combination of energy and luminosity upgrade doubles the mass reach.

14 TeV 100 fb^{-1}	14 TeV 1000 fb^{-1}	28 TeV 100 fb^{-1}	28 TeV 1000 fb^{-1}
4.5	5.4	7.0	9.5

Table 7: 5σ discovery limits for Z' mass in TeV in the $\mu^+\mu^-$ final state for a Z' with the same couplings to quarks and leptons as the Standard Model Z.

The decay $Z' \to WW \to \ell\nu jj$ (see 21.6.1.4 of [1]) has also been studied. This channel is not competitive for discovery but can provide important information on the couplings of the Z'. This study uses the final state where the lepton is a muon as electron detection will be more difficult at higher luminosity. The mass reachable in this final state is shown in Table 8.

	14 TeV 300 fb^{-1}	14 TeV 3000 fb^{-1}	28 TeV 300 fb^{-1}	28 TeV 3000 fb^{-1}
Mass (TeV)	1.9	2.5	2.4	3.3

Table 8: 5σ discovery limits in TeV for a Z' observed in the $WW \to \mu\nu jj$ final state.

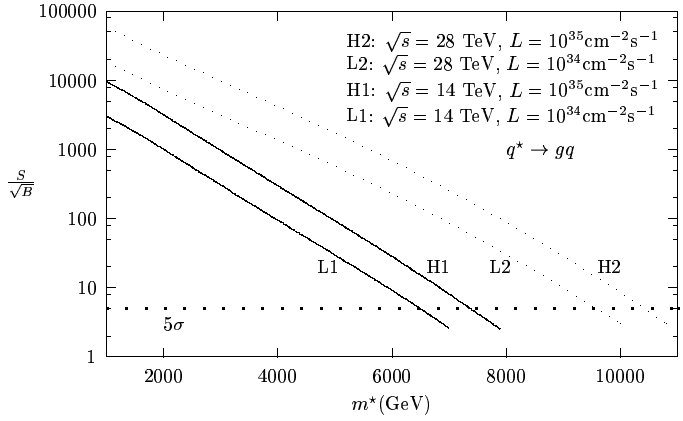

Figure 11: The statistical significance of an excited quark signal as a function of the excited quark mass in the final state $jet + jet$ at 14 and 28 TeV and integrated luminosities of 100 and 1000 fb^{-1}.

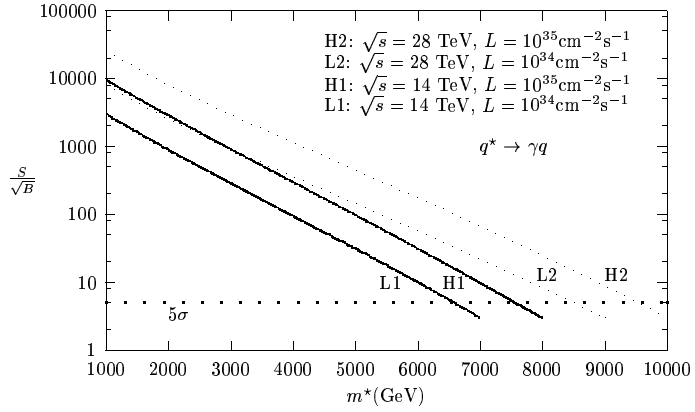

Figure 12: The statistical significance of an excited quark signal as a function of the excited quark mass in the final state $\gamma +$ *jet* at 14 and 28 TeV and integrated luminosities of 100 and 1000 fb^{-1}.

The ability to measure muons and jets of high transverse momenta is needed for these channels which not very sensitive to performance degradations at higher luminosity.

8 Searches for excited quarks

Section 21.3 of Ref [1] and Ref. [10] discuss signals for new exotic quarks. Some of these studies have been repeated for the upgrade exercise. The decays $q^* \to qg$ and $q^* \to q\gamma$ have been simulated. Figures 11 and 12 show the statistical significance of the signal in these channels as a function of the excited quark mass in the $jet - jet$ and $jet - \gamma$ final states. The mass reach increases by about 4 TeV for the highest energy/luminosity configuration. As only jets and photons of the very highest transverse energy are needed in the analysis, this process is rather robust even at the very highest luminosity.

Coupling	14 TeV	14 TeV	28 TeV	28 TeV
	100 fb^{-1}	1000 fb^{-1}	100 fb^{-1}	1000 fb^{-1}
λ_γ	0.0014	0.0006	0.0008	0.0002
λ_Z	0.0028	0.0018	0.0023	0.009
$\Delta\kappa_\gamma$	0.034	0.020	0.027	0.013
$\Delta\kappa_Z$	0.040	0.034	0.036	0.013
g_1^Z	0.0038	0.0024	0.0023	0.0007

Table 9: 59% C.L. constraints on the triple gauge boson couplings

9 Triple gauge-boson couplings

The final state $W\gamma \to \ell\nu\gamma$ ($WZ \to \ell\nu\ell\ell$) has been used to probe the couplings λ_γ and $\Delta\kappa_\gamma$ (λ_Z, $\Delta\kappa_Z$ and g_1^Z) that describe the $WW\gamma$ (WWZ) interaction vertex. More details of the methodology can be found in Section 16.2 of [1]. For a luminosity of 10^{35} cm^{-2} sec^{-1}, the analysis reported here uses only muons and photons. This represents a loss of 50% (75%) of the $W\gamma$ (WZ) effective rate. The constraints on the κ couplings arise primarily from the angular distributions whereas those on the λ couplings arise from the transverse momentum distributions. As only the latter are used here, the results are pessimistic in the case of the κ couplings. The expected sensitivity is shown in Table 9 and the correlations in Fig. 13. Note that both the energy or luminosity upgrades extend the sensitivity for λ_γ into the range (~ 0.001) expected from radiative corrections in the Standard Model and should allow a meaningful test of these corrections and others that arise for example in supersymmetric models.

In contrast to most of the other examples discussed, the luminosity increase is more powerful than the energy increase in this case.

10 Comments and conclusion

There are other processes where some impact from the upgrades can be expected. The Higgs physics program will largely be completed before any upgrade. Some coupling measurements could be limited by statistics and could benefit from an upgrade.

In the case of SUSY Higgs there are regions of parameter space where only one Higgs state (h) will have been seen. In the case of $m_A = 500$ GeV the energy upgrade increases the H/A cross-section by approximately a factor of five thereby increasing the discovery potential for heavy Higgs bosons.

This survey of physics processes at an upgraded LHC enables one to draw certain conclusions. The luminosity upgrade is more limited. Without major detector upgrades, *i.e.* by using only final states of high p_T jets and/or muons, such a luminosity upgrade is expected to provide a $\sim 20\%$ improvement in the mass reach for such physics as SUSY and extra-dimensions. This increase is significant for signals at the limit of the LHC sensitivity. However, the failure of the Inner Detector will compromise electron identification as well as b and hadronic τ tagging. For many new physics processes, statistical samples are improved by combining channels with electrons and muons. In addition valuable information about new physics can be obtained by looking for violation of $e/\mu/\tau$ universality. Pile-up of minimum bias events has severe impact on the ability to use forward jet tagging and central jet vetoing as a tool to enhance signal to background ratios at luminosities significantly higher than 10^{34} cm^{-2} sec^{-1}. Therefore major detector upgrades would be needed to exploit fully the factor of ten increase in luminosity.

The energy upgrade is much easier to exploit. It can significantly enhance the physics reach of the LHC by almost a factor of two in mass. In addition, if new physics is discovered, then the energy upgrade will

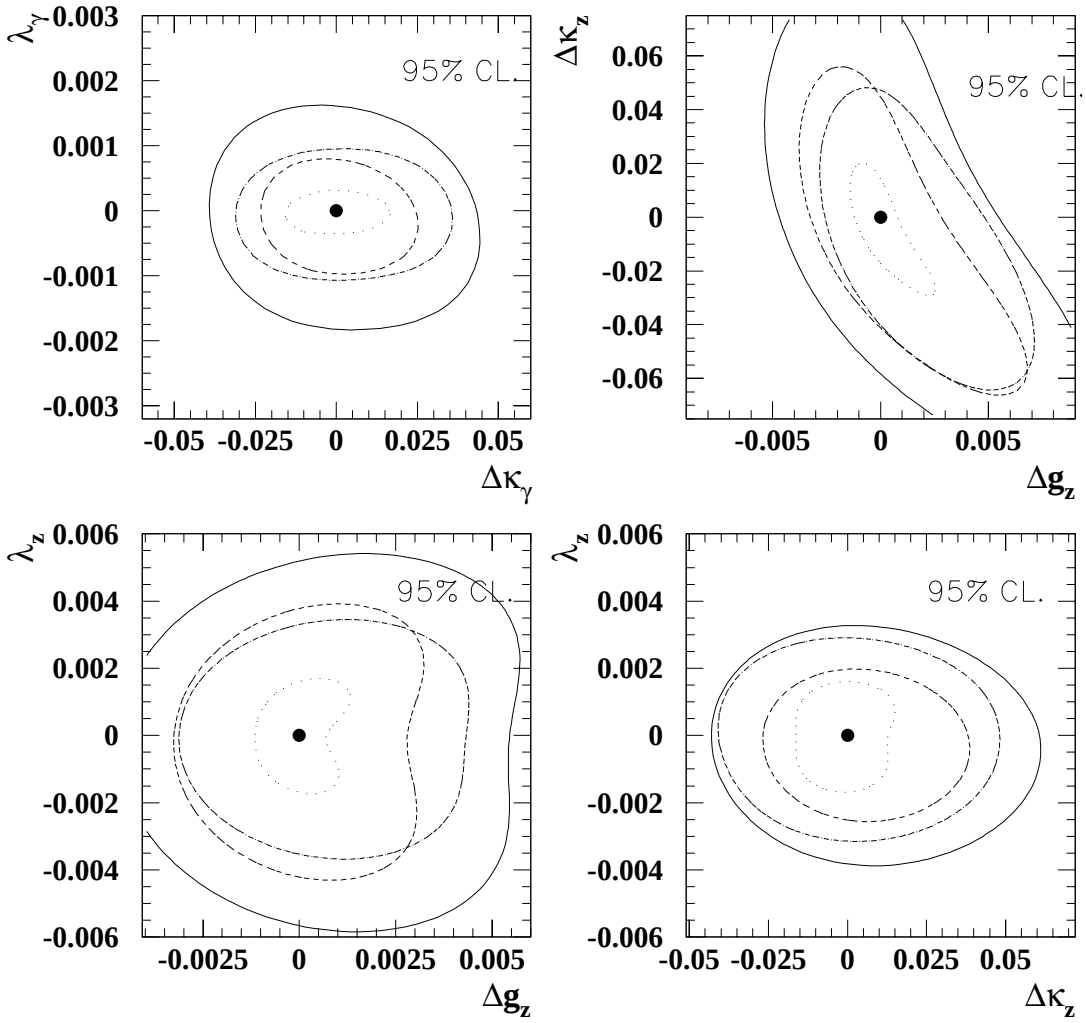

Figure 13: Expected 95% C.L. constraints on triple gauge-boson couplings κ and λ resulting from two parameter fits. The contours correspond to 14 TeV and 100 fb^{-1} (solid), 28 TeV and 100 fb^{-1} (dot dash) 14 TeV and 1000 fb^{-1} (dash) 28 TeV and 1000 fb^{-1} (dotted).

allow significant further study of the new physics. For instance, should supersymmetry be discovered, the production rates for squarks and gluinos are approximately ten times larger at 28 TeV.

References

[1] ATLAS Collaboration, "ATLAS Physics and Detector Performance Technical Design Report," LHCC 99-14/15 (1999).

[2] W.T. Giele *et al.*, Nucl. Phys B403 (1993) 633.

[3] W. Beenakker, R. Hopker and M. Spira, hep-ph/9611232.

[4] H. L. Lai *et al.*, Phys. Rev. **D51**, 4763 (1995) [hep-ph/9410404].

[5] H. Baer, C. Balazs, P. Mercadante, X. Tata and Y. Wang, hep-ph/0008061 (2000)

[6] E. Richter-Was, D. Froidevaux and L. Poggioli, ATL-PHYS-98-131 (1998).

[7] ATLAS Liquid Argon Technical Design Report, CERN/LHCC/96-41 (1996).

[8] M. S. Chanowitz and M. K. Gaillard, Nucl. Phys. **B261** (1985) 379.

[9] L. Vacavant and I. Hinchliffe, hep-ex/0005033 (2000).

[10] O. Cakir, C. Leroy and R. Mehdiyev, Phys. Rev. D **62**, 114018 (2000).